International Journal of Ocean System Engineering 1(3) (2011) 155-164
http://dx.doi.org/10.5574/IJOSE.2011.1.3.155

Second-order Motion Characteristics of a Semi-submersible Platform in Waves†

Sa Young Hong[1*], Bo-Woo Nam[1], Jin-Ha Kim[1], Young-Shik Kim[1], Seok Won Hong[1], and Young-Soo Kim[2]

[1] *Maritime and Ocean Engineering Research Institute, KORDI, Daejeon, KOREA*
[2] *Daewoo Shipbuilding and Marine Engineering, Geoje, KOREA*

(Manuscript Received June 14, 2011; Revised July 8, 2011; Accepted July 27, 2011)

Abstract

The second-order motion characteristics of a semi-submersible are investigated in regular waves. A higher-order boundary element method in a frequency domain and a finite element method in a time-domain were applied to the numerical analysis of the nonlinear hydrodynamic force and motion characteristics of semi-submersibles in view point of potential flow. Various aspects of nonlinear effects on the heave and roll of a semi-submersible were numerically investigated and some selected cases were compared with the model test data.

Keywords: Second-order drift force, Second-order heave motion, Second-order roll motion, Semi-submersible, Time-domain FEM, List angle

1. Introduction

The need to consider the higher-order effect is increasing in the seakeeping analysis of semi-submersible platforms(Semis) because the operational and survival environmental requirements of the Semis are becoming increasingly severer. For this purpose, model tests in harsh wave conditions have been carried out to estimate the seakeeping performance of the Semis since the prediction of seakeeping performance using state of the art numerical tools is not fully capable in extremely harsh environments.

For a deepwater semi-submersible drilling rig operating in a benign sea, the rig has relatively shorter columns and a shallow draft. In such a case, another concern of nonlinear motion analysis has arisen from the nonlinear roll motion presumably induced by second-order roll moment which results in large heeling angle. Voogt et al.[1](2002) observed a steady list angle of a semi-submersible platform in a regular wave at a 180 degree direction in their model test. They found that the steady heeling is mainly induced at specific wave periods when the draft is shallow and the GM is small. Their findings showed that the presence of the current magnifies the list angle and that a threshold wave height occurs which induces the heeling. They numerically showed that a small heeling angle induces a significant increase of roll drift moment. Voogt and Soles[2](2007) revisited the same problem in view of stability.

In the present study, the second-order motion characteristics of a semi-submersible are investigated in regular waves. A higher-order boundary element method(HOBEM) in frequency domain and a finite element method(FEM) in time-domain were applied to a numerical analysis of the nonlinear wave forces and motion characteristics of semi-submersibles in view of potential flow. Various aspects of the nonlinear effects on

* Corresponding author. Tel.: +82-31-400-6000, Fax.: +82-31-400-6079.
E-mail address: syhong@moeri.re.kr.

heave and roll of a semi-submersible were numerically investigated. Some selected cases of model test data were compared with numerical results, which showed complicated behaviors that are difficult explain in terms of potential theory.

2. Formulation of Second-order Boundary Value Problem

The Laplace equation is the governing equation of a potential flow problem associated with floating body dynamics. The body boundary and bottom boundary conditions are implemented by a non-permeable condition. The nonlinearity of surface wave described by the potential flow model is due to free surface and body boundary conditions. Pinkster[3](1980) and Ogilvie[4](1983) have shown a systematic derivation of second-order boundary value problems for a floating body in waves.

The following is a summary of the second-order boundary value problem considered in the present study.

-Governing equations

$$\nabla^2\phi^{(i)} = 0, \quad \text{in } \Omega \tag{1}$$

-Free surface conditions

$$g\eta^{(1)} + \phi_t^{(1)} = 0, \quad \text{in } S_F(z=0) \tag{2}$$

$$\eta_t^{(1)} - \phi_z^{(1)} = 0, \quad \text{in } S_F(z=0) \tag{3}$$

$$g\eta^{(2)} + \phi_t^{(2)} + \frac{1}{2}\left[\left(\phi_x^{(1)}\right)^2 + \left(\phi_y^{(1)}\right)^2 + \left(\phi_z^{(1)}\right)^2\right] + \eta^{(1)}\phi_{tz}^{(1)} = 0, \quad \text{in } S_F(z=0) \tag{4}$$

$$\eta_t^{(2)} - \phi_z^{(2)} + \phi_x^{(1)}\eta_x^{(1)} + \phi_y^{(1)}\eta_y^{(1)} - \eta^{(1)}\phi_{zz}^{(1)} = 0, \quad \text{in } S_F(z=0) \tag{5}$$

where ϕ and η are the velocity potential and wave elevation, respectively. The superscript inside parenthesis denotes the order of magnitude. The subscript denotes derivative with respect to the subscript. Ω and S_F are the fluid domain and free surface, respectively. g is the gravitational acceleration and the normal vector($\vec{n}$) is defined as positive when it is directed into the body.

-Body boundary conditions

$$\frac{\partial\phi^{(1)}}{\partial n} = \vec{n}\cdot\frac{\partial(\vec{\xi}^{(1)} + \vec{\alpha}^{(1)}\times\vec{x})}{\partial t}, \quad \text{on } S_B \tag{6}$$

$$\begin{aligned}\frac{\partial\phi^{(2)}}{\partial n} &= \vec{n}\cdot\frac{\partial(\vec{\xi}^{(2)} + \vec{\alpha}^{(2)}\times\vec{x})}{\partial t} - \\ &\vec{n}\cdot\left(\frac{\partial(\vec{\xi}^{(1)} + \vec{\alpha}^{(1)}\times\vec{x})}{\partial t}\cdot\nabla\right)\nabla\phi^{(1)} \\ &+ \left(\vec{\alpha}^{(1)}\times\vec{n}\right)\cdot\left(\frac{\partial(\vec{\xi}^{(2)} + \vec{\alpha}^{(2)}\times\vec{x})}{\partial t} - \nabla\phi^{(1)}\right) \\ &+ \vec{n}\cdot H\vec{x}, \quad \text{on } S_B\end{aligned} \tag{7}$$

where $\vec{\xi}$ and $\vec{\alpha}$ are the translational and rotational motion vectors, respectively.

It can be easily seen from the above equations that the solution of the first-order problem constitutes a forcing term of the second-order problem. Therefore, the solution of the second-order problem could be obtained by using the solution of the first-order problem.

The incident wave potentials up to the second-order used in the present analysis are defined as follows.

$$\Phi_I^{(1)} = \frac{gA}{\omega}\frac{\cosh k(z+h)}{\cosh kh}\sin(kx - \omega t) \tag{8}$$

$$\Phi_I^{(2)} = \frac{3\omega g A^2}{8}\frac{\cosh 2k(z+h)}{\sinh^4 kh}\sin(2kx - 2\omega t) \tag{9}$$

The second-order forces can be obtained as expressed in Eq.(10)(Ogilvie[4](1983)).

$$\begin{aligned}\vec{F}^{(2)} &= \frac{1}{2}\int_{WL}\left[\eta^{(1)} - \left(\xi_3^{(1)} + \alpha_1^{(1)}y - \alpha_2^{(1)}x\right)\right]^2\vec{n}dl \\ &- \rho\iint_{S_B}\left(\frac{1}{2}\nabla\phi^{(1)}\cdot\nabla\phi^{(1)}\right)\vec{n}dS \\ &- \rho\iint_{S_B}\left[\left(\vec{\xi}^{(1)} + \vec{\alpha}^{(1)}\times\vec{x}\right)\cdot\nabla\phi_t^{(1)}\right]\vec{n}dS \\ &+ \vec{\alpha}^{(1)}\times\vec{F}^{(1)} - \rho\iint_{S_B}\phi_t^{(2)}\vec{n}dS\end{aligned}$$

(10)

$$\vec{M}^{(2)} = \frac{1}{2}\int_{WL}\left[\eta^{(1)} - \left(\xi_3^{(1)} + \alpha_1^{(1)} y - \alpha_2^{(1)} x\right)\right]^2 \vec{r}\times\vec{n}dl - \rho\iint_{S_B}\left(\frac{1}{2}\nabla\phi^{(1)}\cdot\nabla\phi^{(1)}\right)\vec{r}\times\vec{n}dS - \rho\iint_{S_B}\left[\left(\vec{\xi}^{(1)} + \vec{\alpha}^{(1)}\times\vec{x}\right)\cdot\nabla\phi_t^{(1)}\right]\vec{r}\times\vec{n}dS + \vec{\alpha}^{(1)}\times\vec{M}^{(1)} - \rho\iint_{S_B}\phi_t^{(2)}\vec{r}\times\vec{n}dS$$

(11)

3. Numerical and experimental results

3.1Numerical analysis

Numerical analysis was carried out using both frequency domain and time domain methods.

A HOBEM code 'MLINHYDH' was used for analysis of second-order mean forces of which features are as follows(Choi and Hong[5], 2002):

- Bi-quadratic 9-node element
- Generalized multi-body interaction
- Free of irregular frequencies
- Time mean and slowly varying second-order force

A time-domain FEM analysis was conducted for the estimation of second-order motion and force simultaneously. Details of the time-domain FEM can be found in Hong and Nam[6](2010), the technical features of which are summarized as follows:

- An 8-node hexahedral element and a 4-node quadrilateral element
- Linear and 2nd-order free surface condition
- Numerical beach for wave absorption
- 4th-order Adams-Bashforth-Moulton method for free surface time marching, Newmark method for equation of motion

In order to induce roll moment in head sea condition, a small initial heel angle was applied artificially so that the boundary value problem was solved for the heeled geometry both for HOBEM and FEM analysis.

3.2 Model Test

A deepwater semi-submersible drilling rig has been tested at the MOERI Ocean Engineering Basin. It was observed that the so called list angle occurred at specific wave frequency in head sea condition as reported by Voogt et al.[1](2002). The distance between column centerlines is 56m, the outer beam is 73m, and the displacement at operational draft is 38,000 tons. The operating and survival drafts are 17m and 14.5m, respectively. The roll natural periods are 60 and 72 seconds for operating and survival drafts, respectively. 6-dof motion was measured for a series of wave periods from 6 seconds to 24 seconds. At the wave periods of 7 ~ 9 seconds, steady heeling was observed at head sea condition. Outside these wave periods, no significant heeling angle occurred. Additional tests for changing the wave height and adding a current condition were conducted. The same conclusion was drawn as that by Voogt et al. for the effect of current on the list angle. For the wave height effect, it was found that a higher wave height does not always give a larger list angle.

3.3 Numerical and Experimental Results and Discussions

First, the sensitivity of the initial heel angle and heading angle effects on the roll mean drift moment was investigated by changing the initial heel angle from 1 to 3 degrees and the heading angle from 180 to 150 degrees. Fig. 1 shows a panel representation of the semi-submersible at survival draft and Fig. 2 presents the two results. The upper figure shows the effects of the heeling angle and the lower figure shows the effects of the heading angle change. It is notable that a small change of heeling angle induces significantly more roll moment than the change of head-

ing angle of up to 30 degrees off from the head sea. It is also observed that the roll drift moment induced by the initial heel angle appears at specific wave frequencies such as 0.8 and 1.05 rad/s which correspond to multiples of column spacings.

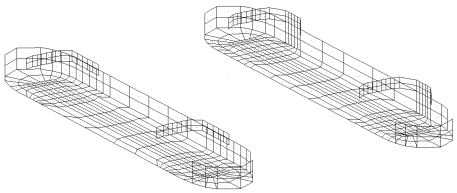

Fig.1 HOBEM mesh

Fig. 3 shows the component of heave and roll drift force and moment. For the heave drift force an even keel mesh was used while 1 degree heeled mesh was used for the roll drift moment calculation. The velocity square contribution is dominant for the vertical mode wave drift forces, which means a small heel angle induces a dramatic change of velocity field between the left and right hand side pontoons even in head sea condition, depending on incident wave period. As shown in Fig. 2, the first peak of roll drift moment occurs at wave frequencies of 0.7 ~ 0.8 rad/s, which corresponds to wave periods of 8 ~ 9 seconds where a remarkable heel angle was observed in the model test. However the second peak occurs at wave frequencies of 1.0 ~ 1.1 rad/s which correspond to wave periods of 5.7 ~ 6.3 seconds where no significant heel angle was observed. Since the so called list angle occurred at relatively short periods of wave, the freely floating motion effect is not significant. Fig. 4 compares the roll drift moment when the motion of the semi is suppressed. No noticeable change was observed between the two cases.

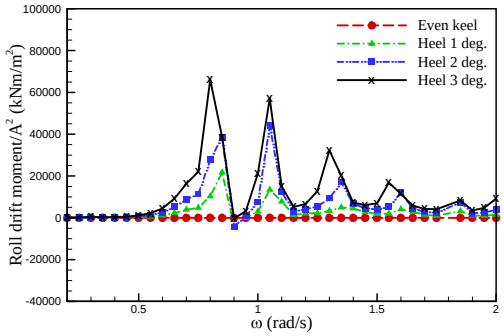

(a) Effects of heel angle (head sea)

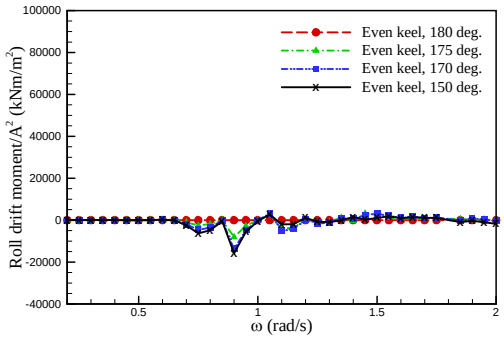

(b) Effects of heading (even keel)

Fig.2 Roll drift moments from HOBEM calculations

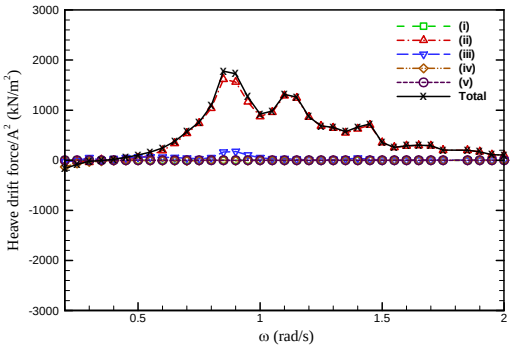

(a) heave drift force at even keel

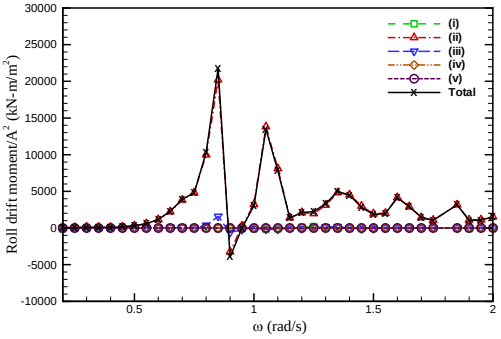

(b) roll drift moment at heel = 1.0 deg.

Fig.3 2nd order component of heave and roll drift forces in head sea.

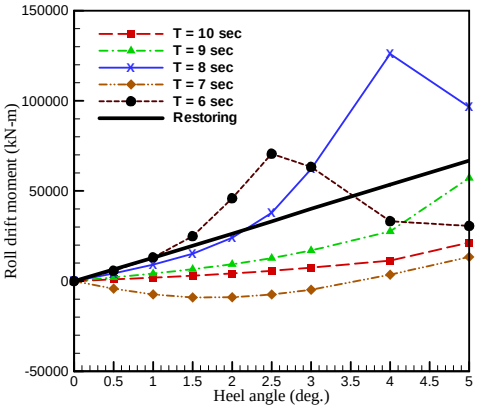

Fig. 5 Roll drift moment with different heel angle

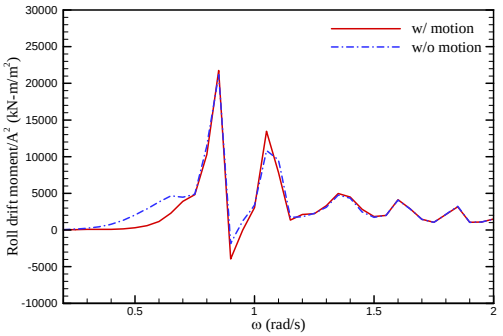

Fig. 4 Effect of motion on roll drift moments

Fig. 5 shows the initial heel angle effects on the roll drift moment for wave periods of 6 ~ 10 seconds. For wave periods of 8 seconds, at which the list angle was clearly observed in the model test, it is notable that the roll drift moment grows as the heel angle increases. For a wave period of 6 seconds, the roll drift moment grows until the initial angle of 2.5 degrees and then subsequently declines. For other wave periods such as 7 and 9 seconds, the qualitative trend is similar to 6 and 8 seconds, but the growing rate is not so significant for the initial heel angle increase.

Typical examples of the nonlinear roll and heave motions of a semi-submersible platform in regular head waves are shown in Fig. 6. The draft was the survival draft. It is observed that a positive upward mean heave motion appears, which is mainly induced due to the heave mean drift force. As shown in Fig. 6(a), the existence of a considerable heave mean drift force seems to have a close correlation with the occurrence of a list angle at head waves. The measured mean upward heave motion also supports close correlation between list angle and heave drift force.

Fig. 6(c) shows the typical list roll phenomenon in head waves. The roll motion has a steady state mean value. The wave period is 8 seconds, which corresponds to the wave period near to which the largest heave and roll mean drift forces occur simultaneously. At wave periods of 6 and 7 seconds, a slowly varying roll motion was observed. Such slowly varying motion could be caused by an unwanted disturbance that is usually negligible for other types of tests. Another explanation can be found in Fig. 5, which shows that the roll drift moment decreases as the roll angle passes the threshold values. In case of a wave period of 6 seconds, the roll drift moment decreases after a heel angle of 2.5 degrees. Such an upper bound of the roll drift moment makes it possible to explain why the roll list angle does not grow after reaching specific list angles of 3 ~ 5 degrees.

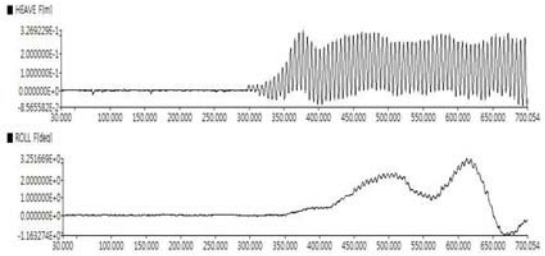

(a) H=2m, T=6sec.

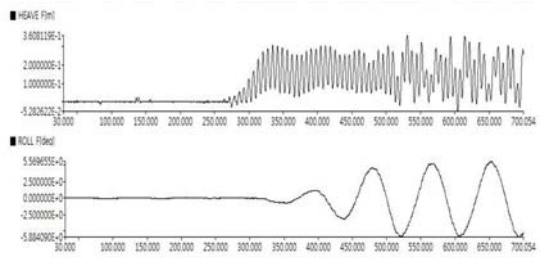

(b) H=2m, T=7 seconds

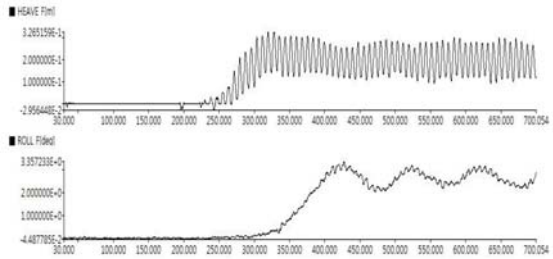

(c) H=2m, T=8 seconds

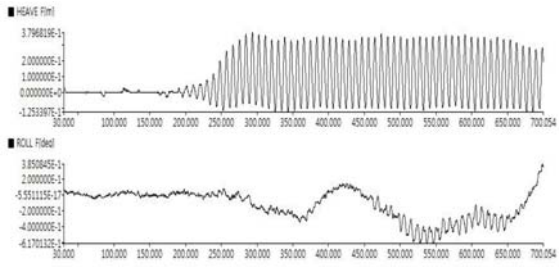

(d) H=2m, T=9 seconds

Fig. 6 Measured roll and heave motion in regular head waves(survival draft)

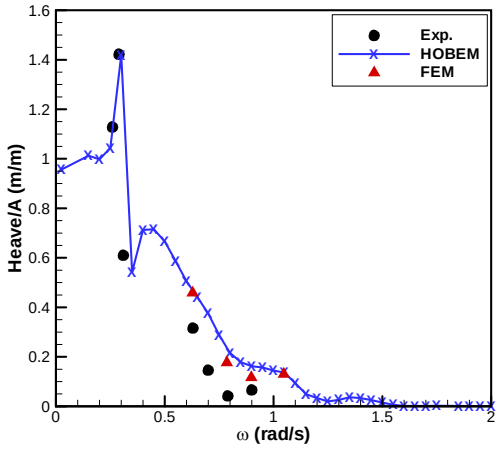

(a) Heave transfer function

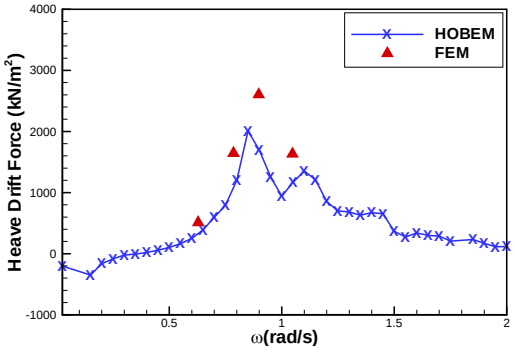

(b) Heave Drift forces

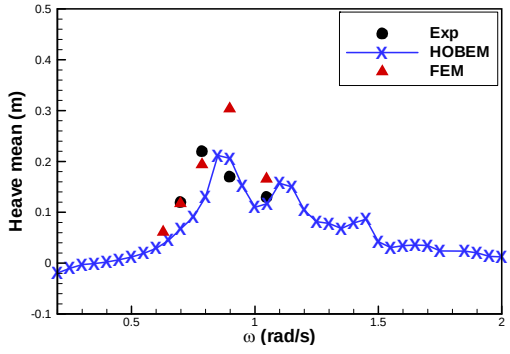

(c) Heave mean offset

Fig. 8 Comparison of heave RAO, drift force and mean offset

Fig. 7 represents the FEM mesh used for time-domain analysis. The heave motion response, heave drift force and heave mean offset are compared with those of HOBEM and the model tests in Fig. 8. Reasonably good agreements between the FEM and the model tests, and the results of the time-domain FEM are verified

Fig. 9 shows FEM analysis results in a form of time series. The wave period is 8 seconds, the heading angle is 180 degrees(head sea) and the wave height is 2m. The initial heel angle was set to be 1 degree. FEM analysis results describe well the nonlinear motion characteristics qualitatively and quantitatively. For heave motion, both the mean offset and linear motion amplitude agree well with the model test results. For roll motion, the mean offset and linear motion characteristics are well described qualitatively, but the mean offset is under predicted compared to the model test result because the FEM analysis uses a frozen mesh based on perturbation nonlinear scheme even if the method accounts for up to the second-order nonlinearity. As previously described, the initial heel angle was 1 degree. The measured mean roll angle was about 2.5 degrees, which coincides with Fig. 5, where the equilibrium of roll mean drift moment with the restoring moment is described.

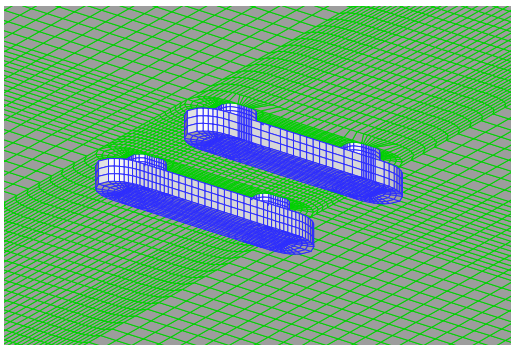

Fig. 7 FEM mesh for semi-submersible platform

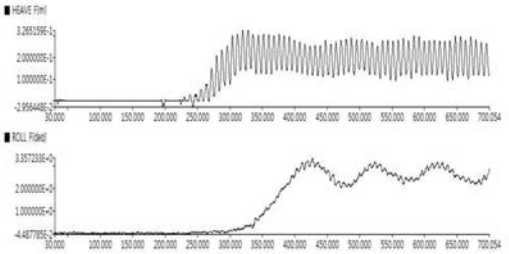

(a) Model test

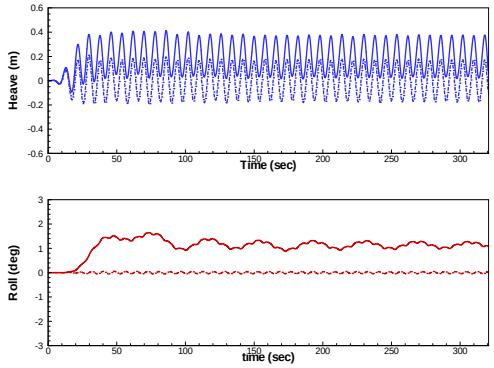

(b) FEM (dash line : 1st only , solid line : 1st + 2nd)

Fig. 9 Comparison of heave and roll motion in head waves, (H=2m, T=8 seconds, survival draft)

Fig. 10 shows another example of FEM analysis for a wave period of 6 seconds in head waves. It is interesting to find that the FEM results also show a larger roll in slow motion amplitude similarly to the model test result.

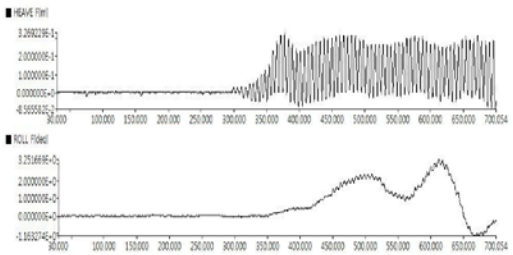

(a) Experiment

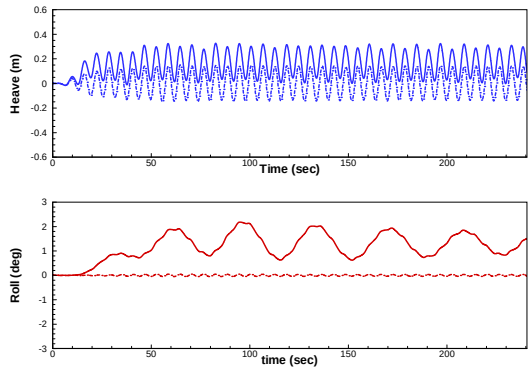

(b) FEM (dash line: 1st only , solid line : 1st + 2nd)

Fig.10 Comparison of heave and roll motion in head waves, (Survival draft, H=2m, T=6seconds)

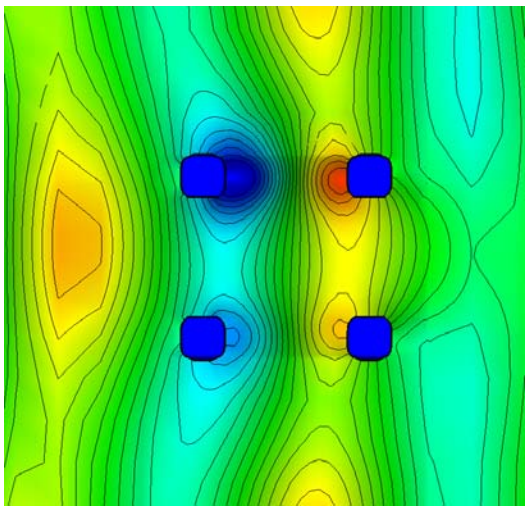

Fig. 11 Total wave contour at t=0.46T (Survival, H=2m, Heel=1.0deg, T=8sec)

Figs. 11 and 12 show the wave contour for the case of a wave period of 8 seconds in head sea condition. Fig. 11 shows the total wave contour at t=0.46T. The incident wave propagates from the right to the left directions in the figure, and the upper columns have a slightly smaller draft due to the initial heel angle. It is clear that the shallower pontoon region shows a strong interaction and such strong interaction resulted in a strong set-down phenomenon at that region. Fig. 12 shows the 2nd-order wave contour at t=0.7T when the set-down effect is considerably highlighted. As shown in Fig. 12, it is clear that the set-down significantly contributed to the roll drift moment.

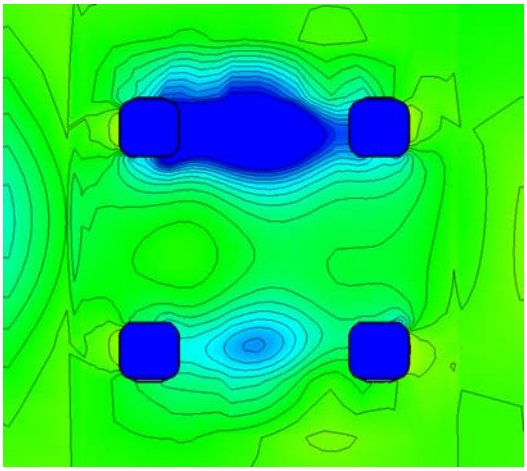

Fig. 12 Second-order scattered wave contour at t=0.7T (Survival, H=2m, Heel=1.0deg, T=8sec)

It has been known that the so called roll list phenomenon is magnified when the current and wave co-exist. Fig. 13 shows such an example; the condition is a head sea, a wave period of 9 seconds, and H=2m, with and without a current.

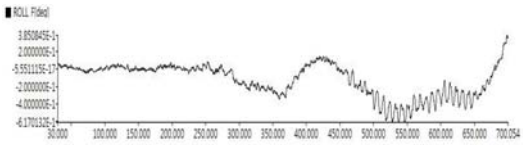

(a) No current

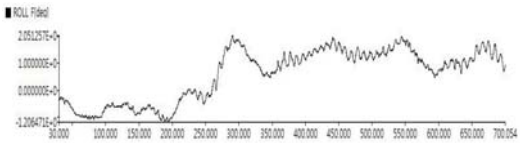

(b) Current: 3 knots

Fig. 13 Effects of current velocity on roll list phenomenon (Head sea, H=2m, T=9 seconds)

As shown in Fig. 14, the current velocity of 3 knots clearly induced a steady roll moment, but

this is not always the case because the adding current occasionally did not increase the mean roll angle and even decreased it. Fig. 15 shows the numerical results of the roll drift moment when the effect of the current is considered. The current effect is considered as an encounter frequency change. As shown in the figure, the added current resulted in a shift of peak frequencies but did not always give an increase of roll drift moment in terms of potential theory.

Another concern for the roll list phenomenon is that a higher wave height does not result in a larger list angle. Fig. 15 compares the measured heave and roll for different wave heights(2m & 6m) but with the same wave period of 8 seconds in head sea condition. As shown in the figure, the linear heave component shows an increase proportional to wave height but the mean offset did not grow proportionally to the wave height square. The heave offset increased by two times, and the roll list angle showed a negligible increase. This result implies that application of the potential theory to the description of the mean and slow motion of roll and heave is limited to moderate wave height because of the shallow water region from the top of the pontoon to the waterline.

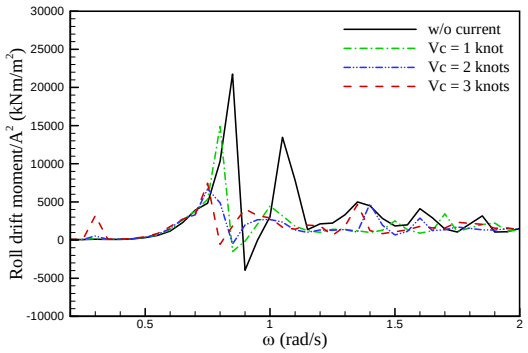

Fig. 14 Effect of current on roll drift moment(head sea, initial heel angle = 1 degree)

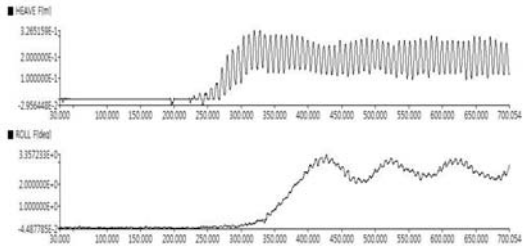

(a) H=2m

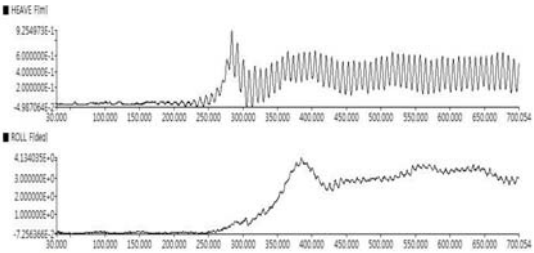

(b) H=6m

Fig. 15 Comparison of heave and roll motion in head waves, (T=8 seconds, survival draft)

4. Conclusions

The nonlinear motion characteristics of a semi-submersible platform at a survival draft in head sea condition were investigated by numerical and experimental methods. The mean heave offset and the so called roll list angle were analyzed using HOBEM in frequency domain and FEM in time domain. Both methods reasonably describe the heave mean offset and the roll list angle in terms of potential theory for moderate wave height. It was numerically found that a small initial angle induces a significant nonlinear roll moment which consequently induces a roll list angle. The time domain FEM results showed that a small initial heel angle induces a significant difference in the set-down effect between the two pontoons, which resulted in a roll list moment.

The effects of increasing wave height and the inclusion of a current speed on the mean

heave and roll motions were not sufficiently described in terms of potential theory because an extremely shallow water region formed due to the large pontoon and the shallow draft induces a highly nonlinear behavior which is beyond the capability of the potential theory.

Acknowledgements

The part of present work is a result of "Development of Extreme Response Analysis Technologies for Offshore Structures" granted by the Korea Research Council of Fundamental Science and Technology. The leading author thanks to DSME for the permission to use model test data.

References

[1] Voogt, AJ, Soles, JJ and Dijk, RV, *Mean and Low Frequency Roll for Semi-submersibles in Waves*, Proc 12th Int. Offshore and Polar Eng Conference, ISOPE, Kita-Kyushu,(2002) pp 379-384

[2] Voogt, AJ and Soles, JJ, *Stability of Deepwater Drilling Semi Submersibles*, Proc 10th Int Symp on Practical Design of Ships and Other Floating Structures, Houston, (2007)

[3] Ogilvie, T.F., *Second order hydrodynamic effects on ocean platforms*, Proc. Intern. Workshop on Ship and Platform Motions, Berkeley, (1983) pp.205-265.

[4] Pinster, J.A., *Low frequency second order wave exciting forces on floating structures*, Netherlands Ship Model Basin, Publication No.650, (1980).

[5] Choi, YR and Hong SY. *An Analysis of Hydrodynamic Interaction of Floating Multi-body Using Higher-Order Boundary Element Method*, Proc 12th Int. Offshore and Polar Eng Conference, ISOPE, Kita-Kyushu, (2002) pp 303-308

[6] Hong, SY and Nam BW. *Analysis of Second-order Wave Force on Floating Bodies Using FEM in Time-domain*, Proc 20th Int. Offshore and Polar Eng Conference, ISOPE, Beijing, (2010).